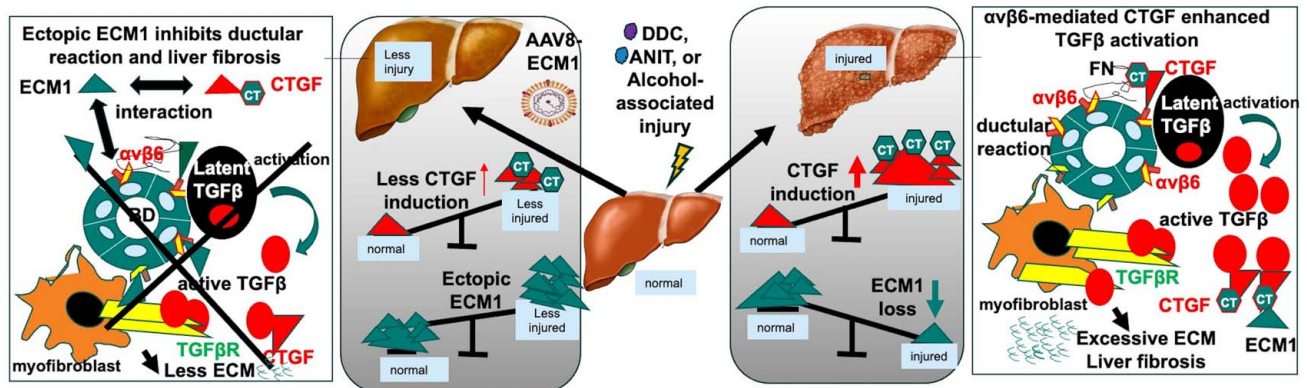


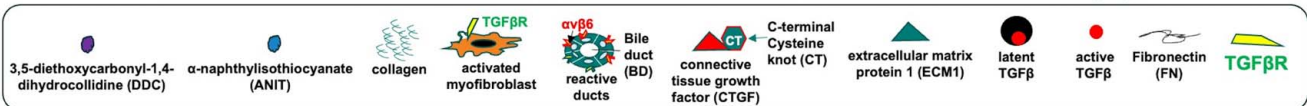
# Extracellular matrix protein 1 binds to connective tissue growth factor against liver fibrosis and ductular reaction

## VISUAL ABSTRACT

### Extracellular matrix protein 1 binds to connective tissue growth factor against liver fibrosis and ductular reaction



**Key Finding:** ECM1 binds to the CT motif of CTGF and inhibits  $\alpha v \beta 6$ -mediated TGF $\beta$  activation thereby leading to attenuated ductular reaction and liver fibrosis after DDC, ANIT, or alcohol-induced liver injury.



## ORIGINAL ARTICLE

OPEN

# Extracellular matrix protein 1 binds to connective tissue growth factor against liver fibrosis and ductular reaction

Chunbao Sun<sup>1</sup> | Weiguo Fan<sup>2</sup> | Sreenivasulu Basha<sup>1</sup> | Tian Tian<sup>1</sup> |  
 Brady Jin-Smith<sup>1</sup> | Joshua Barkin<sup>1</sup> | Hanhui Xie<sup>1</sup> | Junmei Zhou<sup>3</sup> |  
 Xiao-Ming Yin<sup>1</sup> | Chen Ling<sup>4</sup> | Bing Sun<sup>2</sup> | Bryon Petersen<sup>5</sup> | Liya Pi<sup>1</sup>

<sup>1</sup>Department of Pathology, Tulane University, New Orleans, Louisiana, USA

<sup>2</sup>Key Laboratory of Multi-Cell Systems, Shanghai Institute of Biochemistry and Cell Biology, Center for Excellence in Molecular Cell Science, Chinese Academy of Sciences, Shanghai, China

<sup>3</sup>Guangxi Key Laboratory of Molecular Medicine in Liver Injury and Repair, The Affiliated Hospital of Guilin Medical University, Guilin, China

<sup>4</sup>State Key Laboratory of Genetic Engineering and Engineering Research Center of Gene Technology (Ministry of Education), School of Life Sciences, Zhongshan Hospital, Fudan University, Shanghai, China

<sup>5</sup>Department of Pediatrics, University of Florida Gainesville, Florida, USA

## Correspondence

Liya Pi, Department of Pathology, Tulane University School of Medicine, 1430 Tulane Ave, New Orleans, LA 70112, USA.  
 Email: [lp@tulane.edu](mailto:lp@tulane.edu)

## Abstract

**Background:** Extracellular matrix protein 1 (ECM1) can inhibit TGF $\beta$  activation, but its antifibrotic action remains largely unknown. This study aims to investigate ECM1 function and its physical interaction with the profibrotic connective tissue growth factor (CTGF) in fibrosis and ductular reaction (DR).

**Methods:** *Ecm1* knockouts or animals that ectopically expressed this gene were subjected to induction of liver fibrosis and DR by feeding 3,5-diethoxycarbonyl-1,4-dihydrocollidine (DDC) or  $\alpha$ -naphthyl-isothiocyanate (ANIT). ECM1 and CTGF were also examined in the livers of patients with alcohol-associated liver disease (ALD) or ethanol-exposed animals that were fed the western diet for 4 months in the WDA model with liver pathology resembling ALD in patients.

**Results:** ECM1 bound to CTGF in yeast two-hybrid systems, cultured liver cells, and cholestatic livers damaged by DDC or  $\alpha$ -naphthyl-isothiocyanate. This interaction blocked integrin  $\alpha\beta6$ -mediated TGF $\beta$  activation, thereby reducing fibrotic responses in vitro. ECM1 downregulation was associated with biliary CTGF induction during human ALD progression. In experimental models, *Ecm1* loss enhanced susceptibility to DDC-induced cholestasis with upregulation of *Ctgf*,  $\alpha\beta6$ , alpha-smooth muscle actin, procollagen type I, serum transaminase, and total bilirubin levels in germline knockouts, whereas forced expression of this gene significantly attenuated DR and biliary fibrosis after the feeding of DDC or  $\alpha$ -naphthyl-isothiocyanate containing diets. Moreover, ectopic *Ecm1* inhibited not only alcohol-associated fibrosis but also TGF $\beta$ -mediated deregulation of hepatocyte nuclear factor 4 $\alpha$ , preventing the production of the fetal p2 promoter-driven isoforms in the WDA model.

**Abbreviations:** AC, alcohol-associated cirrhosis; AH, alcohol-associated hepatitis; ALD, alcohol-associated liver disease; ANIT,  $\alpha$ -naphthyl-isothiocyanate; CK, cytokeratin; CT, C-terminal cysteine knot; CTGF, connective tissue growth factor; DDC, 3,5-diethoxycarbonyl-1,4-dihydrocollidine; DR, ductular reaction; ECM, extracellular matrix; ECM1, extracellular matrix protein 1; EpCAM, epithelial cell adhesion molecule; HNF4 $\alpha$ , hepatocyte nuclear factor 4 $\alpha$ ; LAP, latent-associated protein; MBP, maltose binding protein; PBC, primary biliary cholangitis; PSC, primary sclerosing cholangitis; RGD, arginylglycylaspartic acid; WDA, western diet with alcohol;  $\alpha$ SMA, alpha-smooth muscle actin.

Supplemental Digital Content is available for this article. Direct URL citations are provided in the HTML and PDF versions of this article on the journal's website, [www.hepcommjournal.com](http://www.hepcommjournal.com).

This is an open access article distributed under the terms of the Creative Commons Attribution-Non Commercial-No Derivatives License 4.0 (CCBY-NC-ND), where it is permissible to download and share the work provided it is properly cited. The work cannot be changed in any way or used commercially without permission from the journal.

Copyright © 2024 The Author(s). Published by Wolters Kluwer Health, Inc. on behalf of the American Association for the Study of Liver Diseases.

**Conclusions:** We uncover a novel antifibrotic action by ECM1 that binds CTGF and inhibits integrin  $\alpha\beta6$ -mediated TGF $\beta$  activation. Targeting its loss has therapeutic potential for the treatment of DR and liver fibrosis in chronic conditions, such as cholangiopathy and ALD.

**Keywords:** alcohol-associated liver disease, ANIT, cholestasis, connective tissue growth factor, DDC, ductular reaction, ethanol, extracellular matrix protein 1, liver fibrosis

## INTRODUCTION

Liver fibrosis, characterized by scar tissue formation, is an abnormal wound healing response common in various chronic liver diseases ranging from viral infection, drug toxicity, alcohol abuse, metabolic dysfunction-associated steatohepatitis, primary sclerosing cholangitis (PSC), and primary biliary cholangitis (PBC).<sup>[1]</sup> Replacement of the functional parenchyma with scar tissue may eventually cause portal hypertension, cirrhosis, liver failure, and even liver cancer. Hepatic progenitor/oval cells can be activated in the form of ductular reaction (DR) during severe liver damage when hepatocytes lose their replicative ability. The expansion of reactive DR-capable cells correlates with the extent of liver fibrosis, and the upregulation of biliary markers, such as cytokeratin (CK) 7 and epithelial cell adhesion molecule (EpCAM), is associated with poor prognosis in alcohol-associated hepatitis (AH).<sup>[2–4]</sup> Currently, liver transplantation is the only treatment option available for patients with end-stage chronic liver disease. Cirrhosis is one of the most common causes of liver transplantation worldwide. There is an urgent need to develop antifibrotic drugs to control the progression of liver fibrosis during reversible stages.

Overproduction of profibrotic signaling promotes HSC activation, leading to excessive matrix production. TGF $\beta$  is a potent cytokine that stimulates extracellular matrix (ECM) formation and the induction of other profibrogenic mediators.<sup>[5]</sup> This protein is typically synthesized as an inactive latent precursor that requires cleavage and/or dissociation from the latent-associated protein (LAP) before engaging with the TGF $\beta$  receptor complex.<sup>[6]</sup> Integrins, such as  $\alpha\beta6$  and  $\alpha\beta8$ , recognize arginylglycylaspartic acid (RGD) tripeptides containing arginine, glycine, and aspartic acid in LAP and activate TGF $\beta$  through mechanical stress or proteolysis-mediated mechanisms.<sup>[6,7]</sup> Dimerized TGF $\beta$  binds to TGF $\beta$  receptors, leading to the phosphorylation and nuclear translocation of the SMAD2/3/4 heterocomplex, which transcriptionally activates fibrosis-related genes, including  $\alpha$ -smooth muscle actin ( $\alpha$ SMA) and connective tissue

growth factor (Ctgf). Ctgf potentiates TGF $\beta$  presentation to cognate receptors and enhances profibrogenic signaling.<sup>[8]</sup> Moreover, Ctgf acts as a scaffold linking integrin to enhance cell adhesion signaling. In human cholangiocarcinoma, Ctgf and  $\alpha\beta6$  receptors are highly expressed and function together to regulate DR and biliary fibrosis in experimental models.<sup>[9]</sup> Overexpression of Ctgf has been found in fibrotic diseases involving virtually every organ system, and inhibition of Ctgf effectively reduced collagen production in HSCs and blocked fibrosis in clinical studies and experimental models.<sup>[10]</sup>

Extracellular matrix protein 1 (ECM1) is an extracellular molecule important for maintaining tissue integrity and function. Mutations in the human ECM1 gene can induce hyaline-like deposits and thickened basal membranes in skin diseases such as lipoid proteinosis and lichen sclerosus.<sup>[11]</sup> Recently, this protein has been identified as a critical factor in maintaining the latency of deposited L-TGF $\beta$  and a gatekeeper for homeostasis in a healthy liver.<sup>[12]</sup> Germline deletion of this gene causes spontaneous activation of TGF $\beta$  signaling, progressive fibrosis, and animal mortality, whereas ectopic *ECM1* expression attenuates carbon tetrachloride-induced liver fibrosis and cirrhosis by inhibiting the TGF $\beta$ /Smad signaling pathway.<sup>[12]</sup> To date, the role of *ECM1* in chronic liver disease, DR, and alcohol-induced liver injury is poorly understood. Here, we reported a novel antifibrotic action of Ecm1, which bound to and inhibited profibrotic Ctgf during DR and liver fibrosis. Negative correlations between ECM1 and CTGF were found in AH, PBC, and PSC human livers. *Ecm1* deficiency promoted DR and liver fibrosis, whereas ectopic expression of *Ecm1* attenuated these processes in cholangiopathy induced by  $\alpha$ -naphthyl-isothiocyanate (ANIT) or 3,5-diethoxycarbonyl-1,4-dihydrocollidine (DDC). Ectopic Ecm1 also helped protect murine livers from alcohol-associated fibrosis caused by the feeding of western diet (WD; 40% calories from fat) and alternate 10%–20% ethanol exposure, which is known as the “western diet with alcohol (WDA)” model with induced liver pathology resemble of alcohol-associated liver disease (ALD) in patients.<sup>[13]</sup>

## METHODS

### Human tissue and animal experimentation

Human liver samples with alcohol-associated steatosis, alcohol-associated steatohepatitis, and alcohol-associated cirrhosis (AC) were ordered from Sekisui XenoTech (Kansas City, KS) and subjected to histological analyses and western blotting. These studies used deidentified samples with exempt from Tulane University Institutional Review Board. Human gene expression was analyzed in indicated public data sets. For ectopic expression in AAV8 virus, mouse *Ecm1* [NM\_007899] containing C-terminal FLAG epitope sequences was purchased from Origene (Rockville, MD) and inserted to replace eGFP at NotI and BamHI sites after thyroxine-binding globin promoter in the pAAV. thyroxine-binding globin.PI.eGFP.WPRE.bGH plasmid (Watertown, MA). AAV8-GFP was administered as a control in parallel studies. These viruses were administered at a dose of  $5 \times 10^{11}$  genome particles/mouse into C57BL6 mice (8-wk-old). DR was triggered by 0.1% DDC (Bio-Serv, Frenchtown, NJ) containing diets previously reported by us.<sup>[9]</sup> Cholestasis was also induced by employing an ANIT (0.1%) containing diet, according to Joshi et al.<sup>[14]</sup> The WDA model was performed according to Schonfeld et al.<sup>[13]</sup> C57BL6/J wild-type mice (Jackson Lab, Harbor, ME) were fed a western diet ad libitum (Research Diets, New Brunswick, NJ). Alternated alcohol drinking between 20% v/v (4 d, Thursday through Sunday) and 10% v/v (3 d, Monday through Wednesday) was given for 20 weeks after the animals received progressively increasing amounts of alcohol in water (1%, 3%, 10%, 15%, and 20% v/v for 3 d each). Only 20% v/v alcohol was given during the last 2 weeks of western diet feeding. Molecular characterization of animal models, including RNA isolation and reverse transcriptase-PCR analyses, western analyses, and immunoprecipitation assays, are all described in Supplemental Materials and Methods, <http://links.lww.com/HC9/B62>. Research on mice was approved by the Animal Care and Usage Committee at Tulane University and conducted in compliance with their guidelines. The care of animal and licensing guideline under which the study was performed and report these in accordance with the ARRIV (Animals in Research: Reporting In Vivo Experiments).

### Histological analysis, morphometry, and fibrosis measurement

Histology and immunofluorescent staining were performed with standard protocols. All mouse liver tissues were fixed in 4% paraformaldehyde in PBS. The mouse, normal human, and AC human livers were embedded in paraffin and sectioned in 6  $\mu$ m thickness. Immunohistochemistry (IHC) was performed with anti-A6 (a kind gift from Dr. Valentina Factor at NCI), rabbit anti-Ki67

(Leica), rabbit anti-Ctgf (Abcam, Waltham, MA), chimeric human anti-integrin  $\alpha$ v $\beta$ 6 ch2A1 (Biogen Idec, Cambridge, MA), rabbit anti- $\alpha$ SMA (Proteintech, Rosemont, IL), and mouse anti-CK19 (DSHB, Troma III) followed by detection with DAB, Vector blue or red substrates (Vector Laboratories, Newark, CA) according to our previous report.<sup>[9]</sup>

A laser spinning confocal microscope (Leica TCS SP2, Wetzlar, German) with Velocity software (PerkinElmer, Waltham, MA) was used to visualize immunofluorescence signals. Bright-field images were visualized using a light microscope with the accompanying software. DR and bile epithelia proliferation were indicated by a ratio between the number of CK19<sup>+</sup> Ki67<sup>+</sup> cells versus the total number of CK19<sup>+</sup> bile duct epithelia from images ( $\times 200$  magnification). To evaluate fibrosis, liver sections were stained with Picrosirius red solution (American MasterTech Scientific, St Lodi, CA) or  $\alpha$ SMA antibody followed by detection with Vector blue substrate (Vector Laboratories). The approximate borders of positively stained areas in each periportal field were traced, and the corresponding areas were measured in pixels using ImageJ software. Total positive areas were calculated as a percentage of total pixels in each image. To obtain statistical significance in all the morphometric analyses, at least 10 random-field images were taken per slide, and 4 animals per group were scored. ImageJ software (<http://rsb.info.nih.gov/ij/>) and IHC profiler according to published methods.<sup>[15]</sup>

### Hepatic hydroxyproline, serum, and tissue analyses

Hepatic hydroxyproline content was quantified calorimetrically in flash-frozen murine liver samples. Concentrations were calculated from a standard curve using pure hydroxyproline (Sigma, Saint Louis, MI) and expressed as micrograms of hydroxyproline per gram of livers. Total bilirubin, ALT, and AST were measured from serum according to our previous report<sup>[9]</sup> using commercially available assay kits according to the manufacturer's instructions (Sigma).

### ECM1-CTGF interaction by yeast two-hybrid analyses, solid phase binding assays, immunoprecipitation assay, and proximity ligation assay

Construction of the rat complementary DNA (cDNA) library specific for regenerating livers following 2-acetylaminofluorene (AAF) and partial hepatectomy (PHx) was reported.<sup>[16]</sup> ECM1 and CTGF interaction was characterized in yeast two-hybrid analyses, solid-phase binding assay, immunoprecipitation assay, and proximity ligation assay as described in Supplemental Materials and Methods, <http://links.lww.com/HC9/B62>.

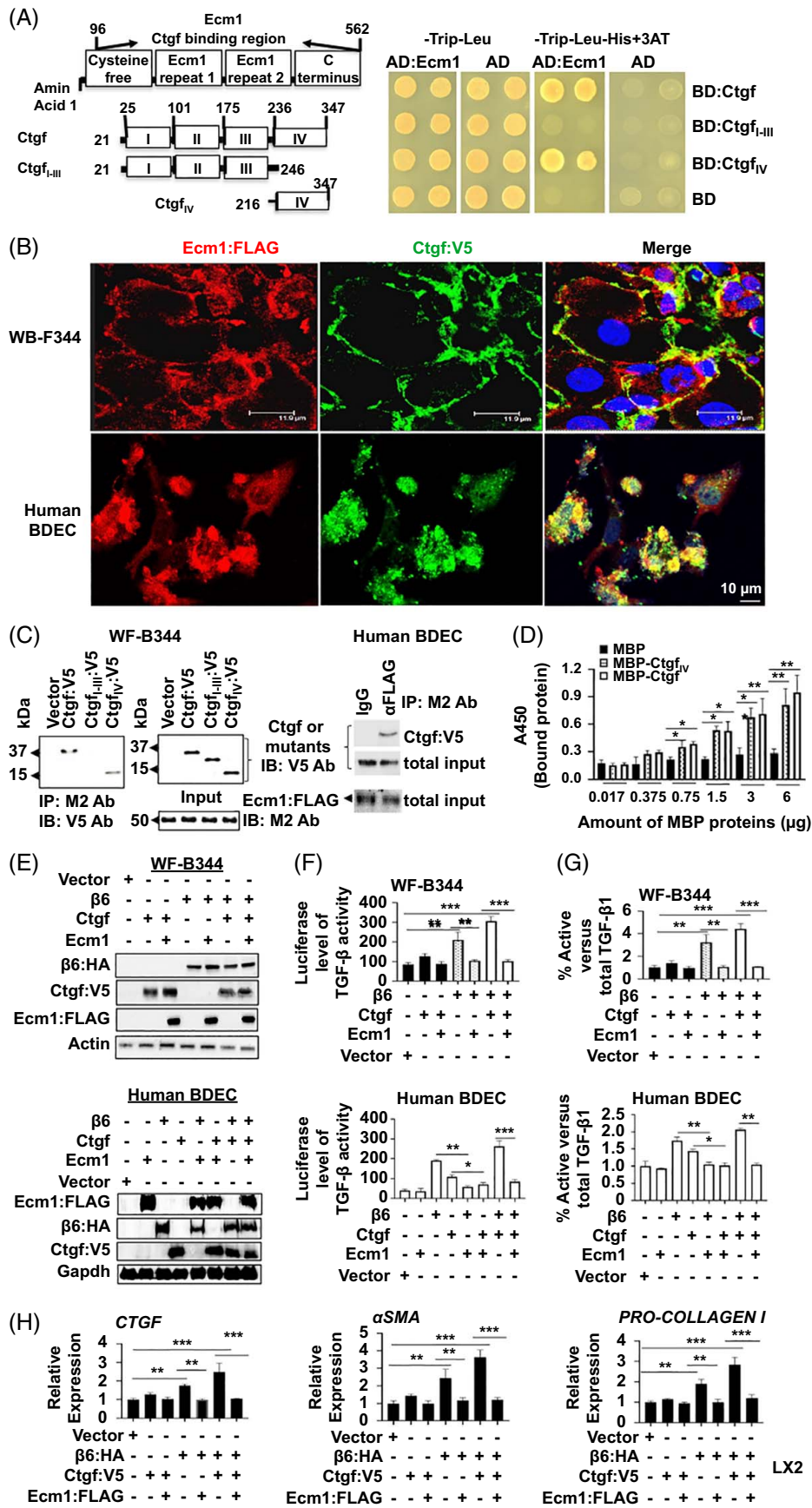


**FIGURE 1** Ecm1 binds to Ctgf and reduces  $\alpha\text{v}\beta\text{6}$ -mediated TGF $\beta$  activation leading to attenuated fibrosis in vitro. (A) Yeast two-hybrid analyses showed that all co-transformants expressing AD and BD constructs grew on permissive media but only the ones containing interactors (Ecm1 with Ctgf or the CtgfIV mutant) could survive on selective media (with 3-AT but lacking leucine, tryptophan, and histidine). (B) The immunofluorescent staining showed colocalization between Ecm1:FLAG and Ctgf:V5 fusion proteins in transfected WB-F344 cells and primary human BDEC. (C) M2 antibody (Ab) that recognized the Ecm1:FLAG protein specifically pulled down Ctgf:V5 and CtgfIV:V5 proteins from conditioned media of the rat hepatic progenitor WB-F344 cells, whereas no immunoprecipitation signal was seen from CtgfI-III:V5 or vector control in immunoprecipitation assays (left). M2 Ab rather than mouse IgG controls could also pull down Ctgf:V5 from the human BDEC lysates (right). Equal input of tested proteins was shown. (D) Dose-dependent binding of MBP-Ctgf or CtgfIV fusion proteins to recombinant ECM1:FLAG protein was detected by M2 Ab-conjugated HRP in solid-phase assays. MBP protein only showed background signal. Values were represented means  $\pm$  SD.  $**p < 0.01$ ;  $*p < 0.05$ . Student *t* test. (E) Western blotting detected the expression of  $\beta\text{6}$ :HA, Ctgf:V5, and Ecm1:FLAG in established WB-F344 stable cell lines and the human BDEC. (F and G) Ecm1 reduced  $\alpha\text{v}\beta\text{6}$ -mediated and Ctgf-potentiated TGF- $\beta$ 1 activation in the WB-F344 stable cell lines and the human BDEC based on plasminogen activator inhibitor 1-driven luciferase activity in co-cultured transfected mink lung epithelial cell (F) and ELISA from the conditioned media of these cells (G). (H) Presence of Ecm1:FLAG significantly reduced the expression of CTGF,  $\alpha\text{SMA}$ , and COLLAGEN genes in LX-2 cells that were exposed to conditioned media containing  $\beta\text{6}$ :HA with or without Ctgf:V5. Values in (F–H) are means  $\pm$  SD from triplicate experiments.  $***p < 0.001$ ;  $**p < 0.01$ ;  $*p < 0.05$  in Student *t* test. Abbreviations: AD, activation domain; BD, binding domain; BDEC, bile ductular epithelial cell; CTGF, connective tissue growth factor; ECM1, extracellular matrix protein 1; HA, hemagglutinin; MBP, maltose binding protein;  $\alpha\text{SMA}$ ,  $\alpha$ -smooth muscle actin.

## TGF $\beta$ 1 Bioassay

TGF $\beta$ 1 activity was measured according to our previous report.<sup>[9]</sup> Detailed characterizations were described in Supplemental Materials and Methods, <http://links.lww.com/HC9/B62>.

## Statistical analysis

GraphPad Prism 6.0 (GraphPad Software, San Diego CA) was used for statistical analysis. Statistical significance ( $p < 0.05$ ) was evaluated using the unpaired *t* test and one-way ANOVA.

## RESULTS

### Ecm1 binds to Ctgf and reduces $\alpha\text{v}\beta\text{6}$ -mediated TGF $\beta$ activation, leading to attenuated fibrotic responses in vitro

Hepatic oval cells can be activated in the form of DR as an alternative pathway for liver regeneration when hepatocyte proliferation is inhibited.<sup>[16]</sup> We identified Ecm1 as a CTGF-binding protein after screening a yeast two-hybrid library specific for oval cell activation and liver regeneration following AAF/PHx in rats.<sup>[17]</sup> The identified clone contained a cDNA fragment covering nucleotide sequences starting at 288 bp to the stop codon (NM\_053882), which encodes a truncated rat Ecm1 protein lacking the first 32 amino acids but containing the rest of the cysteine-free domain, Ecm1 repeat 1, Ecm1 repeat2, and the C-terminal domain (Figure 1A). When this cDNA fragment was expressed in a fusion protein containing the GAL4 activation domain, the resulting Ecm1 fusion protein could interact with Ctgf that was fused to the GAL4 DNA-binding domain because the co-transformants allowed yeast growth in triple selective SD media lacking Histidine,

Leucine, and Tryptophan in the presence of 5 mM 3-amino-1,2,4-triazol, a competitive inhibitor to control stringency for HIS transcription. Further analyses using deletion mutants suggested that the C-terminal cysteine knot (CT) domain (Ctgf<sub>IV</sub>), rather than domains I–III that correspond to insulin-like growth factor binding domain, von Willebrand factor type C motif, thrombospondin type I module in Ctgf, was sufficient for Ecm1 binding. This CT region is implicated in heparin binding and dimerization, and carries known adhesive and proliferative functions for Ctgf signaling.<sup>[18]</sup> To further test this interaction, we expressed FLAG-tagged Ecm1 and V5-tagged Ctgf proteins in WB-F344 cells, a rat hepatic progenitor cell line, and primary human bile ductular epithelial cells (BDECs). Immunofluorescent staining detected the colocalization of Ctgf:V5 and Ecm1:FLAG in the pericellular regions of the co-transfected cells (Figure 1B). Further immunoprecipitation assays showed that Ecm1:FLAG protein could be specifically pulled down from cell lysates containing V5-tagged Ctgf and the Ctgf<sub>IV</sub> mutant but not from the vector control and a truncated mutant containing only domains I–III of Ctgf (Figure 1C). Ctgf:V5 and Ecm1:FLAG were also colocalized and specifically interacted with each other in the human BDEC (Figure 1B). Additionally, the ability of the CT domain of Ctgf for binding to Ecm1 was tested using solid-phase assays. In this assay, maltose binding protein (MBP)-fused Ctgf (MBP:Ctgf) or CT mutants (MBP:Ctgf<sub>IV</sub>) were purified from DE3 *Escherichia coli* and coated on plastic surfaces. Dose-dependent binding was observed in these fusion proteins, whereas the MBP control yielded only background signals (Figure 1D). These results indicated that Ecm1 physically interacts with Ctgf via the CT motif.

Ecm1 protein has been shown to directly bind  $\alpha\text{v}$  integrin and competitively inhibit the interaction between  $\alpha\text{v}$  integrin and the latent precursor of TGF $\beta$ .<sup>[19]</sup> Ctgf binding to  $\alpha\text{v}$  containing integrins ( $\alpha\text{v}\beta\text{6}$ ,  $\alpha\text{v}\beta\text{3}$ ,  $\alpha\text{v}\beta\text{1}$ , etc.) has also been reported.<sup>[9,20,21]</sup> We took advantage of a unique system for detection of extracellular

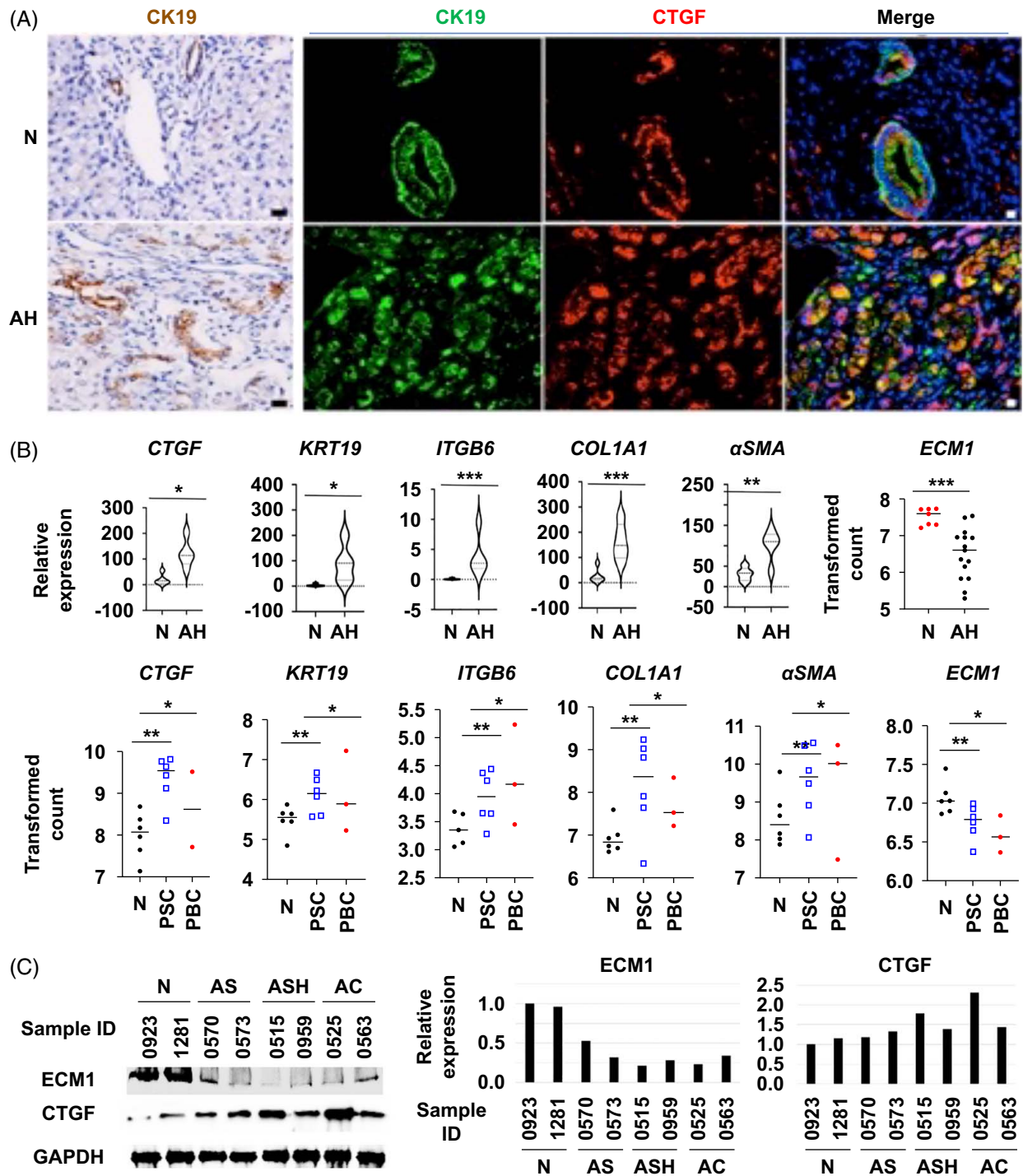


**FIGURE 2** ECM1 loss is associated with Ctgf induction in ductular reaction and liver fibrosis during human chronic liver disease progression. (A) immunohistochemical analysis detected extensive ductular reaction positive for CTGF in reactive ducts of human AH livers compared to normal (N) livers. Scale bar: 100  $\mu$ m. (B) Upregulation of biliary and fibrosis markers including CTGF transcript (from the public data set GSE143318) was associated with loss of ECM1 in human AH livers (from the public data set GDS4389 and GSE143318), PSC and PBC livers (from GSE159676). \*\* $p < 0.01$ ; \* $p < 0.05$  in Student  $t$  test. (C) Western blotting and densitometric analyses indicated the loss of ECM1 and induction of CTGF proteins in livers of patients with AS, ASH, and AC compared to healthy livers ( $n = 2$  per group). Abbreviations: AC, alcohol-associated cirrhosis; AH, alcohol-associated hepatitis; AS, alcohol-associated steatosis; ASH, alcohol-associated steatohepatitis; CTGF, connective tissue growth factor; ECM1, extracellular matrix protein 1; PBC, primary biliary cholangitis; PSC, primary sclerosing cholangitis;  $\alpha$ SMA,  $\alpha$ -smooth muscle actin.

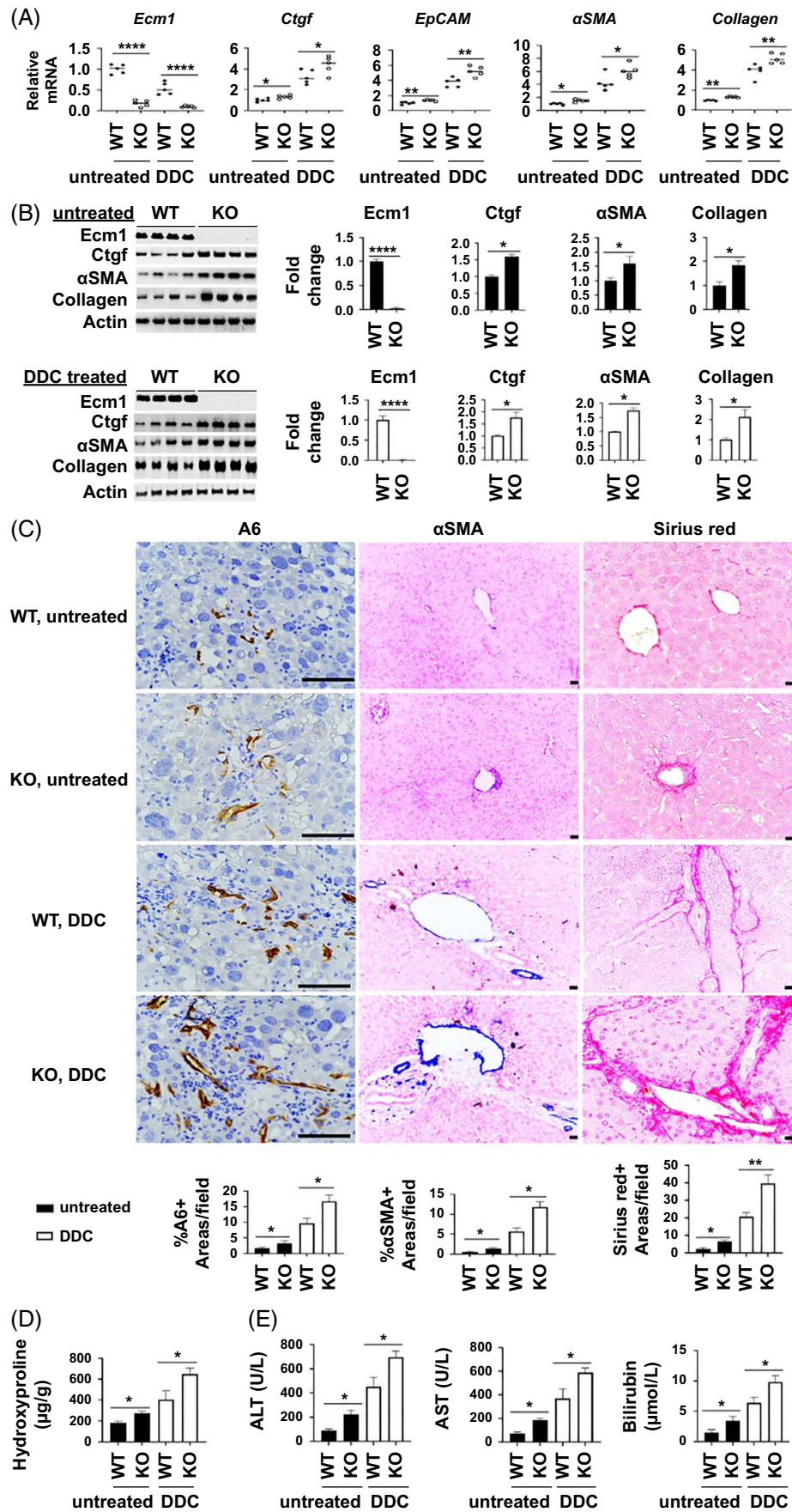




**FIGURE 3** *Ecm1* deficiency promotes biliary fibrosis and DR during DDC-induced liver damage. *Ecm1* KO or WT littermates (7-week-old,  $n=4$ ) were fed 0.01% DDC-containing diet for 5 days. quantitative reverse transcriptase-PCR analyses (A), Western blotting with densitometric analysis (B), and immunohistochemical analysis (C) detected elevated levels of biliary markers and fibrosis-related genes in KO compared to WT littermates in untreated conditions and after DDC feeding.  $\alpha$ SMA was detected with Vector blue substrates. Relative expressions were calculated in comparison to WT livers ( $n=4$ –5/group). Data were represented as means  $\pm$  SEM.  $**p < 0.01$ ;  $*p < 0.05$ . Student *t* test. Graphs are quantification of stained areas based on image analysis of at least 10 random fields ( $\times 200$  magnification) per liver. Scale bar: 100  $\mu$ m. (D and E) The loss of *Ecm1* was associated with elevated levels of hepatic hydroxyproline content (D) and liver injury markers (E) in KO ( $n=4$ ) compared to WT ( $n=5$ ). Data were represented as means  $\pm$  SEM.  $*p < 0.05$ . Student *t* test. Abbreviations: CTGF, connective tissue growth factor; DDC, 3,5-diethoxycarbonyl-1,4-dihydrocollidine; ECM1, extracellular matrix protein 1; KO, knockout;  $\alpha$ SMA,  $\alpha$ -smooth muscle actin; WT, wild type.

interactions by generating biotinylated receptors in which ectodomains were fused with a Cd4d3+4 tag at their C-terminal region according to Sun et al.<sup>[22]</sup> The resulting biotinylated  $\alpha$ v ectodomain, Ctgf:V5, *Ecm1*:FLAG, or in combinations were expressed in WB-F344 cells (Supplemental Figure S1A, <http://links.lww.com/HC9/B62>). We found that Ctgf:V5 or *Ecm1*:FLAG fusion proteins could specifically be pulled down by streptavidin-conjugated beads, whereas these associations with the biotinylated  $\alpha$ v ectodomains were largely reduced when the 2 molecules were overexpressed together (Supplemental Figure S1B, <http://links.lww.com/HC9/B62>). These observations implicated that *Ecm1* and Ctgf interaction was strong and disrupted their individual associations with the  $\alpha$ v containing complexes.

Integrin  $\beta 6$  combines with  $\alpha$ v and forms a heterodimer, specifically in epithelial cells, including cholangiocytes.<sup>[23]</sup> We have shown that integrin  $\alpha\beta 6$  and Ctgf function cooperatively to promote DR during liver damage.<sup>[9]</sup> To determine whether the *Ecm1* interaction with Ctgf influenced  $\alpha\beta 6$ -mediated TGF $\beta 1$  activation in vitro, plasmids expressing these molecules were transfected into the WB-F344 cells and the human BDEC, respectively (Figure 1E). Luciferase activity under the control of the plasminogen activator inhibitor 1 promoter in transfected mink lung epithelial cells was used to measure the degree of TGF $\beta 1$  activation. *Ecm1* significantly inhibited TGF $\beta 1$  activation that was promoted by  $\alpha\beta 6$  integrin and Ctgf in the WB-F344 cells and the human BDEC (Figure 1F). A decreased ratio of active to total TGF $\beta 1$  protein in conditioned media was also observed in the 2 cell types (Figure 1G). Accordingly, conditioned media from the WB-F344 cells expressing  $\alpha\beta 6$  and Ctgf showed the highest induction of *Ctgf*,  $\alpha$ SMA, and *procollagen type I* mRNAs in human HSC LX2 cells. Crucially, the presence of *Ecm1*:FLAG in the conditioned medium significantly reduced these fibrotic responses (Figure 1H). To further understand the regulation of this antifibrotic activity, we inhibited the rat *Ctgf* expression by siRNA in the WB-F344 cell line that was stably expressed *Ecm1*:FLAG and  $\beta 6$ :HA (Supplemental Figure S2A, <http://links.lww.com/HC9/B62>). We found that decreased levels of Ctgf protein were associated with lower TGF $\beta 1$  activation as measured in luciferase assays compared to Scramble siRNA controls (Supplemental Figure S2B, <http://links.lww.com/HC9/B62>), implicating a higher inhibitory activity by *Ecm1* in the presence of low amounts of

Ctgf protein. Similar results were found when we knocked down *CTGF* in the human BDEC using siRNAs that were reported previously.<sup>[24]</sup> Taken together, these results indicate that *Ecm1* binds to Ctgf and inhibits  $\alpha\beta 6$ -mediated Tgf $\beta 1$  activation, leading to the attenuation of fibrotic responses in vitro.

### Induction of biliary and fibrosis markers, including CTGF correlates with ECM1 loss in human AH, PSC, and PBC

ALD consists of liver pathologies ranging from steatosis, AH, fibrosis to AC. DR is another histological feature in advanced ALD.<sup>[2–4]</sup> Subpopulations of patients with AH can develop cholestasis and biliary fibrosis.<sup>[25]</sup> Therefore, we examined the correlation of *ECM1* with biliary and fibrosis-related genes, including CTGF, in normal and diseased livers of patients with ALD, PSC, and PBC. As shown in Figure 2A, IHC detected specific localization of CK19 in the normal bile ducts of human livers, while this biliary cell marker was highly induced in reactive ducts lacking typical lumens in the livers of patients with AC. CTGF was co-expressed with CK19 in the normal human bile ducts and became highly upregulated in the reactive ducts of human AC livers (Figure 2A), supporting our previous report on the critical role of this profibrotic molecule in DR.<sup>[9]</sup> As shown in Figure 2B, the upregulation of *CTGF* and other fibrotic and biliary genes (*COL1A1*, *ITG $\beta 6$* , and *KRT19*) was associated with the downregulation of *ECM1* mRNA in human AH (based on data extracted from GSE143318 and GDS4389 data sets), PSC and PBC (GSE159676/GPL6244 data set). These patterns are consistent with a recent report about the induction of CTGF by Yes-associated protein in the livers of patients with PSC.<sup>[26]</sup> Negative correlations between *ECM1* and CTGF were also confirmed by western blotting using liver homogenates from patients with alcohol-associated steatosis, alcohol-associated steatohepatitis, and AC (Figure 2C).

To further understand cell types that express *CTGF* and *ECM1*, we extracted data from the Human Protein Atlas and found differential levels of these transcripts in normal human liver cells. As shown in Supplemental Figure S3, <http://links.lww.com/HC9/B62>, *CTGF* showed basal expression in vascular smooth muscle

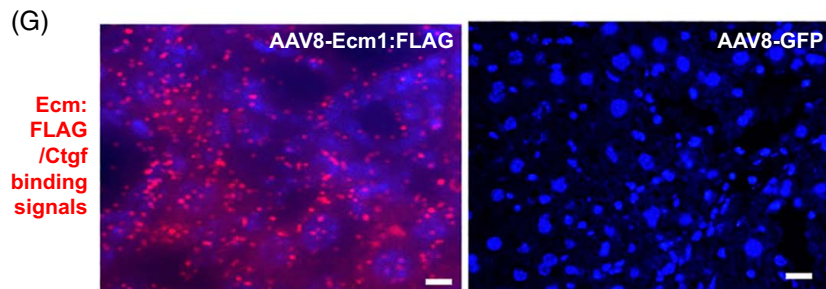
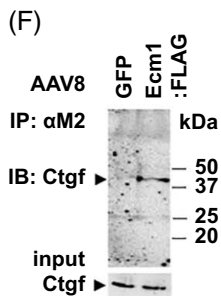
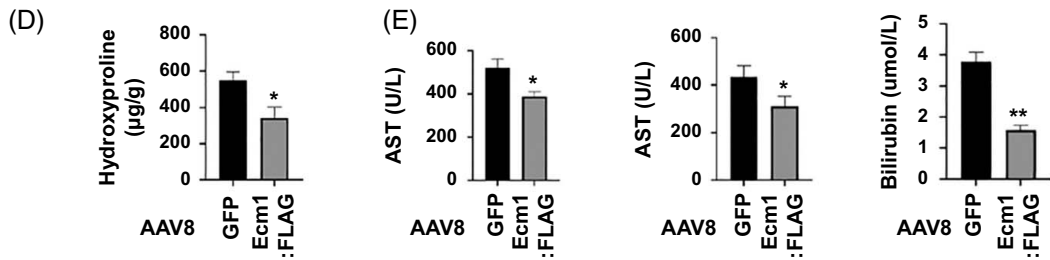
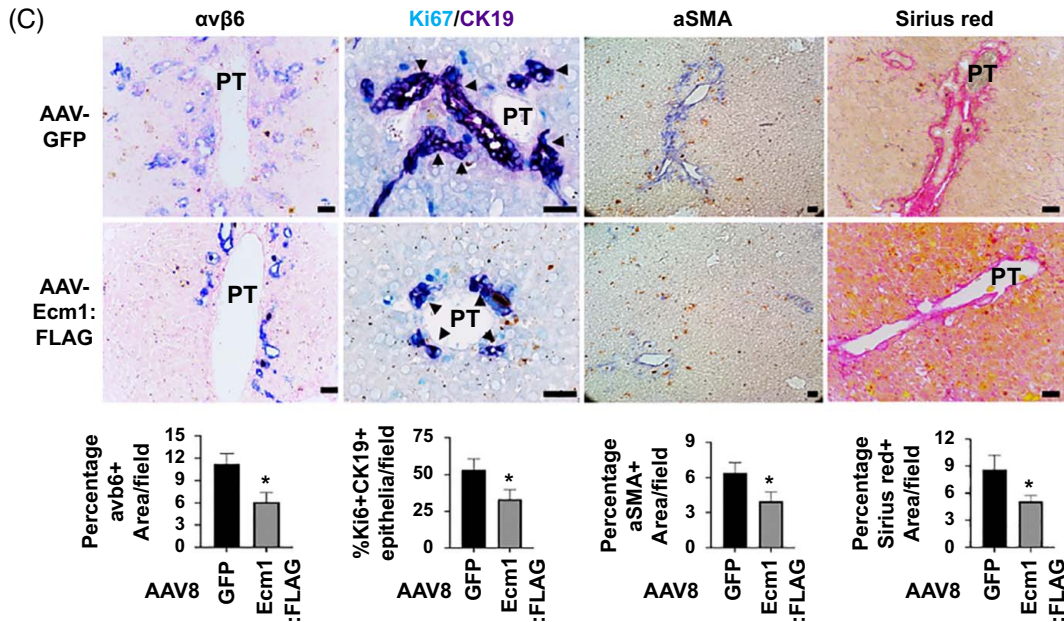
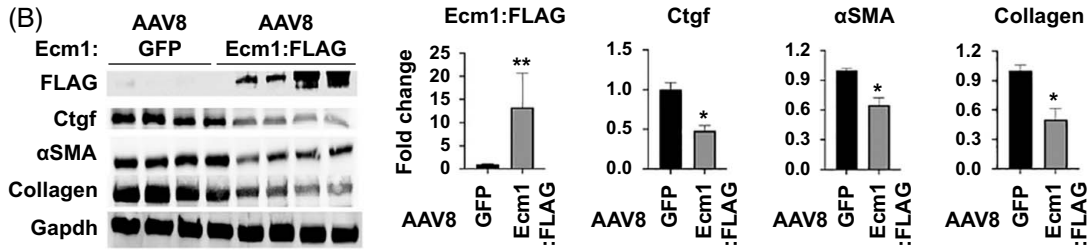
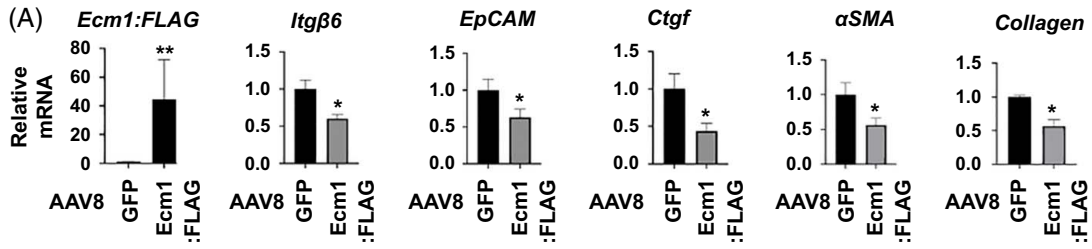


**FIGURE 4** *Ecm1* binds to *Ctgf* and reduces biliary fibrosis and DR during DDC-induced liver damage. Ectopic expression of *Ecm1* in AAV8 virus caused downregulation of biliary markers and fibrosis-related genes at 14 days after DDC feeding shown in quantitative reverse transcriptase-PCR analyses (A), Western blotting with densitometric analyses (B), and immunohistochemical analysis (C). Dual staining were carried out using rabbit anti-Ki67 and mouse anti-CK19 antibodies followed by detection with Vector blue and Vector red substrates respectively. Integrin  $\alpha\text{v}\beta\text{6}$  and  $\alpha\text{SMA}$  were also detected by Vector blue. Sirius red staining was performed to label collagen deposit. Relative expressions were calculated in relation to GFP livers. Data were represented as means  $\pm$  SEM ( $n=4/\text{group}$ ).  $**P < 0.01$ ;  $*P < 0.05$ . Student *t* test. Scale bar: 200  $\mu\text{m}$ . Graphs are quantification of stained areas based on image analysis of at least ten random fields (200x magnification) per animal. Ectopic *Ecm1* also decreased hepatic hydroxyproline content (D) and serum levels of liver injury markers (E). Data were expressed as means  $\pm$  SEM ( $n=4/\text{group}$ ).  $*p < 0.05$ . Student *t* test. (F) Immunoprecipitation assays using M2 antibody pulled down *Ctgf* in the *Ecm1*:FLAG expressing livers. Equal *Ctgf* was input in the assays. (G) Proximity ligation assay detected *Ecm1*:FLAG and *Ctgf* interaction (red signal) on liver sections from animals that received AAV8-*Ecm1*:FLAG or AAV8-GFP infection and 14-day 3,5-diethoxycarbonyl-1,4-dihydrocollidine feeding. Scale bar: 50  $\mu\text{m}$ . Abbreviations: CTGF, connective tissue growth factor; ECM1, extracellular matrix protein 1;  $\alpha\text{SMA}$ ,  $\alpha$ -smooth muscle actin.

cells, endothelial cells, fibroblast cells, and cholangiocytes, whereas low expression was found in hepatocytes and KCs. In contrast, the highest levels of *ECM1* transcripts were in fibroblast cells and endothelial cells while modest expressions were in vascular smooth muscle cell, KCs, cholangiocytes, and hepatocytes. These data are consistent with multiple single-cell RNA analyses of clinical and experimental samples in which *Ecm1* is enriched in quiescent HSCs.<sup>[27–30]</sup> In single-cell transcriptomics data sets related to fibrotic niches of human liver cirrhosis<sup>[31]</sup> and  $\text{CCl}_4$ -induced murine liver fibrosis,<sup>[32]</sup> we found decreased *ECM1* in mesenchymal myofibroblast fractions of cirrhotic human livers (Supplemental Figure S4A–D, <http://links.lww.com/HC9/B62>), and HSC fractions of peaked  $\text{CCl}_4$ -induced fibrotic livers compared to normal controls (Supplemental Figure S5A–D, <http://links.lww.com/HC9/B62>). Hepatocytes in the cirrhotic human livers concomitantly upregulated *CTGF* mRNA in the single-cell RNA analyses (Supplemental Figure S6A–D, <http://links.lww.com/HC9/B62>). These results confirmed the loss of *ECM1* and induction of *CTGF* transcripts during liver fibrosis and cirrhosis in clinical samples and experimental models.

### ***Ecm1* knockouts are susceptible to DR and biliary fibrosis induced by the DDC diet**

*Ecm1* is critical for normal liver function since its germline KO mice die at around 8 weeks of age with spontaneous liver fibrosis, hyperactivation of  $\text{TGF}\beta$ , and abnormal biliary network with DR.<sup>[12]</sup> Consistent with these findings, we found elevated mRNA and protein levels of *Ctgf*, *EpCAM*,  $\alpha\text{SMA}$ , and *procollagen type I* in 7-week-old untreated KO mice compared to those in age-matched wild-type littermates (Figure 3A, B). To understand the roles of murine *Ecm1* in DR and cholangiopathy, we utilized the biliary toxin DDC, which inhibits heme biosynthesis and causes significant porphyria, leading to bile duct obstruction and large duct disease. The DDC model has been widely used to induce DR to study the underlying mechanisms of xenobiotic-induced cholangiopathies and biliary fibrosis in mice.<sup>[33]</sup> DDC caused

gradual loss of *Ecm1* and upregulation of *Ctgf*,  $\alpha\text{SMA}$ , and procollagen type I proteins in wild-type mice during the time course of 3-week feeding (Supplemental Figure S7, <http://links.lww.com/HC9/B62>). Moreover, DDC-induced DR and fibrosis were enhanced in the KO mice compared to wild-type controls as detected by quantitative reverse transcriptase-PCR, western blotting, and IHC (Figure 3A–C). These changes were associated with concomitant increases in hepatic hydroxyproline content and liver injury markers (ALT, AST, and total bilirubin) in the untreated KO mice compared to wild-type controls, while DDC feeding promoted these increases in the *Ecm1*-deficient livers (Figure 3D, E). These data demonstrate that *Ecm1* deficiency enhances the liver susceptibility to cholestasis during DDC-induced injury.

### **Ectopic *Ecm1* binds to *Ctgf* and attenuates DDC-induced DR and biliary fibrosis**

Considering that *Ctgf* can function together with the integrin  $\alpha\text{v}\beta\text{6}$  receptor to promote DR and biliary fibrosis,<sup>[9]</sup> we hypothesized that *Ecm1* binding affected *Ctgf* and integrin  $\alpha\text{v}\beta\text{6}$  activity, thereby interfering with DDC-induced DR and biliary fibrosis. Indeed, AAV8-*Ecm1*:FLAG-infected livers exhibited significantly lower levels of *EpCAM*, *Itgb6*, *Ctgf*,  $\alpha\text{SMA}$ , and *procollagen type I* compared to AAV8-GFP-infected controls at 14 days after DDC feeding (Figure 4A). This ectopic expression of the *Ecm1*:FLAG protein caused a decrease in *Ctgf* protein to 48.32%,  $\alpha\text{SMA}$  to 61.21%, and procollagen type I to 50.82% in western blotting (Figure 4B). Double staining for Ki67 and CK19 showed that the percentage of proliferating biliary epithelial cells reduced from 50.21% in AAV8-GFP-infected livers to 30.58% in AAV8-*Ecm1*:FLAG-infected livers (Figure 4C), indicating DR attenuation. Moreover, reduced fibrosis was observed based on decreased percentages of  $\alpha\text{SMA}^+$  areas ( $4.27 \pm 0.49$  in *Ecm1*:FLAG livers vs.  $6.12 \pm 1.05$  in AAV8-GFP-infected controls,  $p < 0.05$ ) and Sirius red-stained areas for collagen deposition ( $5.00 \pm 0.42$  in the AAV8-*Ecm1*:FLAG-infected livers vs.  $8.70 \pm 1.29$  in AAV8-GFP-infected controls,  $p < 0.05$ ) (Figure 4C). Decreased levels of hepatic hydroxyproline

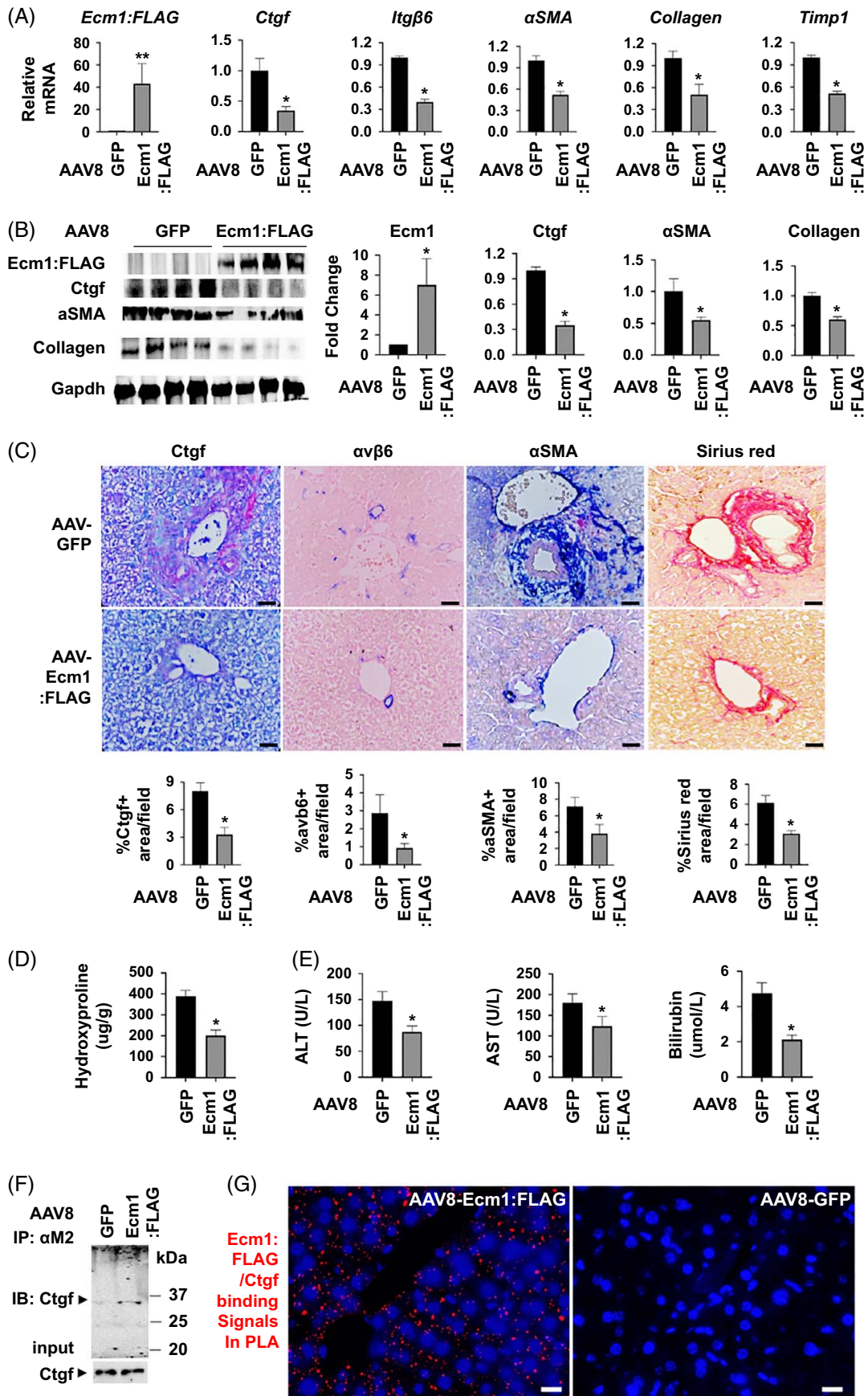


**FIGURE 5** Ecm1 binds to Ctgf and attenuates the ANIT-induced biliary fibrosis. Quantitative reverse transcriptase-PCR analyses (A), Western blotting with densitometric analyses (B), and immunohistochemical analysis (C) showed that ectopic expression of Ecm1 in AAV8 virus could downregulate expression of *Itgβ6*, *Ctgf*,  $\alpha$ SMA, and procollagen type I genes at 1 month after the  $\alpha$ -naphthyl-isothiocyanate feeding. Relative expressions were calculated in comparison to AAV8-GFP-infected controls. Data were represented as means  $\pm$  SEM ( $n=4$ /group). \*\* $p < 0.01$ ; \* $p < 0.05$ . Student *t* test. Scale bar: 100  $\mu$ m. Graphs are quantification of stained areas based on image analyses of at least 10 random fields ( $\times 200$  magnification) per liver. Ectopic expression of Ecm1 gene also decreased levels of hepatic hydroxyproline content (D) and liver injury markers (E) compared to the GFP controls ( $n=4$ ). Data are represented as means  $\pm$  SEM. \* $p < 0.05$ . Student *t* test. (F) Immunoprecipitation assays using M2 antibody pulled down Ctgf in the  $\alpha$ -naphthyl-isothiocyanate damaged, Ecm1:FLAG expressing livers. Equal input of Ctgf was also shown. (G) Proximity ligation assay assays detected direct binding between Ecm1:FLAG and Ctgf proteins (red signal) on liver sections from mice that received AAV8-Ecm:FLAG or GFP infection before the one-month  $\alpha$ -naphthyl-isothiocyanate feeding. Scale bar: 50  $\mu$ m. Abbreviations: CTGF, connective tissue growth factor; ECM1, extracellular matrix protein 1;  $\alpha$ SMA,  $\alpha$ -smooth muscle actin.

and liver injury markers were also found in the livers of DDC-fed mice that ectopically expressed Ecm1:FLAG protein (Figure 4D, E). In addition, M2-conjugated beads that recognized the Ecm1:FLAG protein pulled down Ctgf protein in homogenates of DDC-damaged livers from the AAV8-Ecm1:FLAG-infected mice, but not the AAV8-GFP-infected controls (Figure 4F). Moreover, we used the Duolink proximity ligation assay technology to visualize the interaction between the Ecm1:FLAG and Ctgf proteins, as indicated by the red signal in the AAV8-Ecm1:FLAG-infected livers (Figure 4G). In contrast, only a background signal was observed in the AAV8-GFP-infected controls. These results demonstrate that Ecm1:FLAG protein interacts with Ctgf and reduces DDC-induced DR and biliary fibrosis.

### Ectopic *Ecm1* binds to Ctgf and attenuates ANIT-induced DR and biliary fibrosis

ANIT induces DR and biliary fibrosis.<sup>[34]</sup> This chemical is transported as a glutathione conjugate into the bile, where it selectively damages cholangiocytes and causes cholangiopathy to model human intrahepatic cholestasis. ANIT-induced injury to intrahepatic cholangiocytes can activate a coagulation cascade and induce integrin  $\alpha$ v $\beta$ 6 to promote liver fibrosis.<sup>[35]</sup> We examined the effects of forced *Ecm1* expression on ANIT-induced liver injury response. C57BL/6/J wild-type mice received tail vein injections of AAV8-Ecm1:FLAG or AAV8-GFP, followed by 0.01% ANIT feeding for 1 month. Ectopic expression of Ecm1:FLAG protein was associated with a 62.01% reduction in *Ctgf*, 59.23% in *Itgβ6*, 47.31% in  $\alpha$ SMA, 41.98% in *procollagen type I*, and 40.52% in *TIMP metalloproteinase inhibitor 1* mRNAs compared to AAV8-GFP-infected controls in quantitative reverse transcriptase-PCR analysis (Figure 5A). Western blotting confirmed parallel decreases in Ctgf,  $\alpha$ SMA, and collagen type I protein levels in ANIT-treated livers expressing Ecm1:FLAG (Figure 5B). IHC revealed strong Ctgf,  $\alpha$ SMA, and collagen deposition in onion-ring-like fibrotic lesions of the ANIT-treated AAV8-GFP-infected control livers, whereas these patterns were largely diminished in the AAV8-Ecm1:FLAG-infected livers (Figure 5C). The percentage of stained areas for  $\alpha$ v $\beta$ 6<sup>+</sup> reactive ducts also

markedly decreased in livers expressing Ecm1:FLAG protein ( $0.841 \pm 0.078$  in AAV8-Ecm1:FLAG-infected livers versus  $2.88 \pm 0.815$  in GFP controls,  $p < 0.01$ ) (Figure 5C). Hydroxyproline contents also decreased in the AAV8-Ecm1:FLAG-infected livers ( $196.75 \pm 15.65$   $\mu$ g/g in the Ecm1:FLAG expressing livers versus  $391.25 \pm 20.93$   $\mu$ g/g in the GFP controls,  $p < 0.05$ ) (Figure 5D). Lower levels of ALT further provide evidence of alleviated liver injury ( $86.51 \pm 11.31$  U/L in the sera of the Ecm1:FLAG livers vs.  $147.25 \pm 17.33$  U/L in the GFP controls,  $p < 0.05$ ), AST ( $123.75 \pm 19.28$  U/L in the Ecm1:FLAG sera vs.  $179.5 \pm 18.05$  U/L in the GFP controls,  $p < 0.05$ ), and Bilirubin ( $1.98 \pm 0.13$   $\mu$ mol/L in the Ecm1:FLAG sera vs.  $4.52 \pm 0.63$   $\mu$ mol/L in the GFP controls,  $p < 0.05$ ) (Figure 5E), indicating a protective role of Ecm1:FLAG against ANIT-induced liver injury and biliary fibrosis. To test whether Ecm1:FLAG interacted with Ctgf protein, we performed co-immunoprecipitation assays using total protein lysates from ANIT-damaged livers that were infected with AAV8-Ecm1:FLAG or AAV8-GFP. As expected, the Ctgf protein was specifically pulled down by beads conjugated with an M2 antibody against the FLAG epitope from the AAV8-Ecm1:FLAG-infected livers but not from the AAV8-GFP controls (Figure 5F). In addition, the interaction between Ecm1:FLAG and Ctgf was confirmed with the Duolink proximity ligation assay signals in the AAV8-Ecm1:FLAG-infected livers but not in the AAV8-GFP control livers (Figure 5G). These data demonstrate that ectopic Ecm1 expression inhibits biliary fibrosis, likely by interacting with and sequestering the profibrotic Ctgf protein.

### Ectopic *Ecm1* reduces alcohol-associated fibrosis in the WDA model

Chronic alcohol consumption can cause AH with activation of TGF $\beta$ 1 that serves as a key upstream transcriptome regulator, and induces p2 promoter of hepatocyte nuclear factor (Hnf)4 $\alpha$ , resulting in defective metabolic and synthetic functions in hepatocytes.<sup>[36]</sup> The p1 promoter of Hnf4 $\alpha$  is expressed in adult livers, and the p2 promoter specifically drives gene transcription in fetal livers. The TGF $\beta$ 1 mediated Hnf4 $\alpha$  p1 and p2 imbalance and AH liver pathology can be mimicked

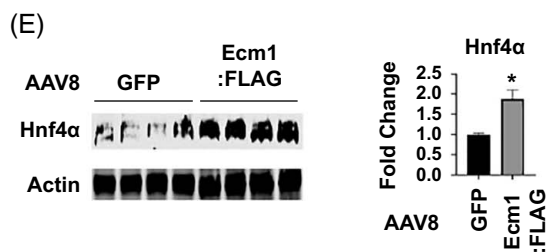
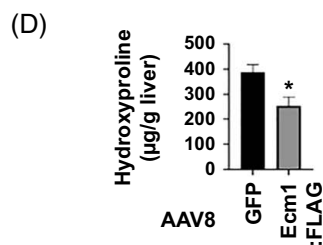
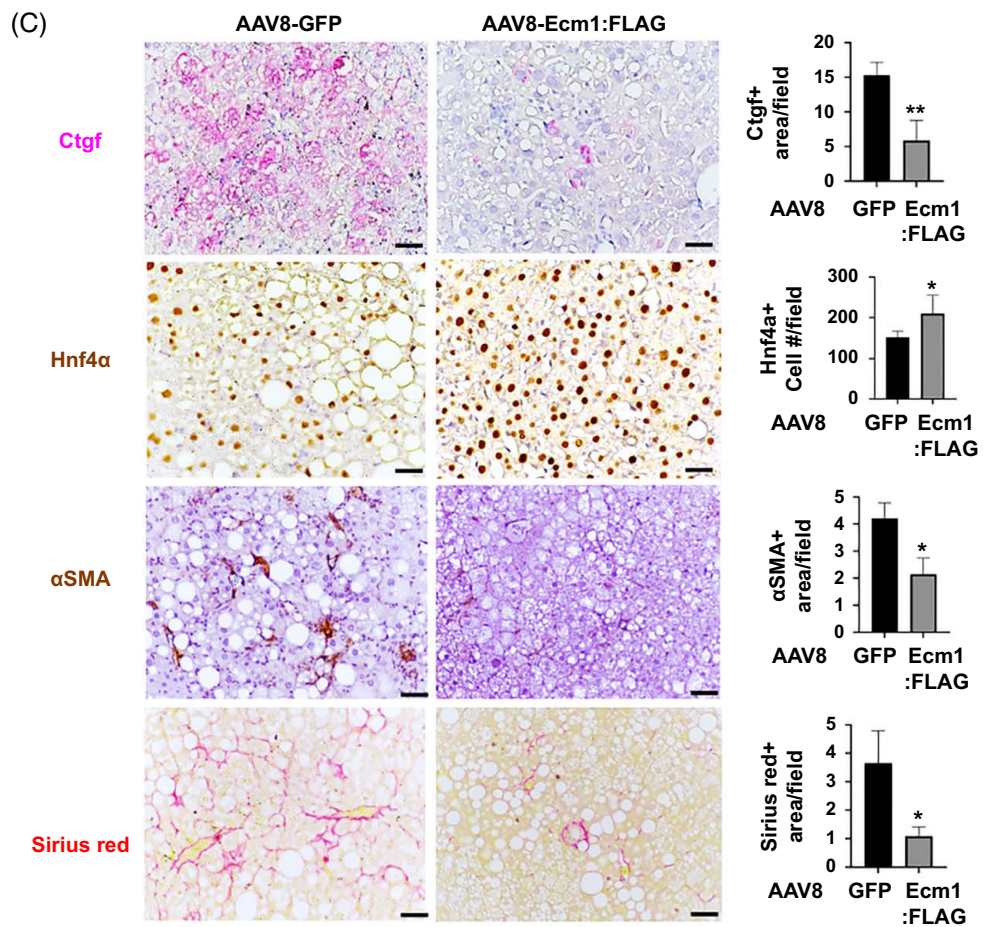
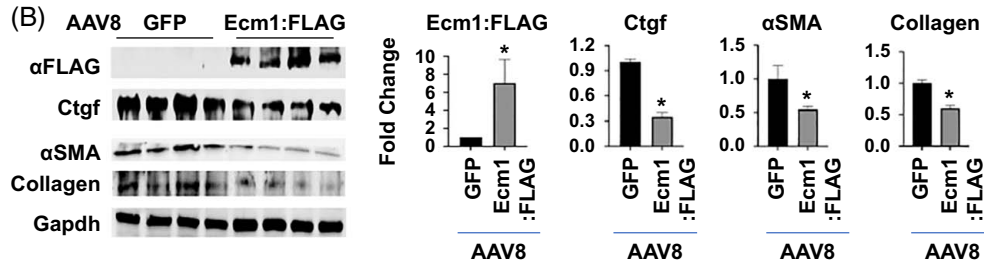
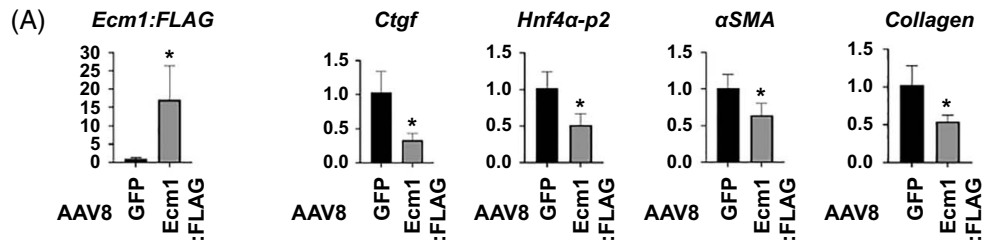


**FIGURE 6** Forced expression of *Ecm1* reduces fibrosis during the WDA-induced liver injury. Q-RT-PCR analyses (A), western blotting with densitometric analysis (B), and immunohistochemical analysis (C) showed lower induction of *Ctgf*, a *Hnf4 $\alpha$ -p2* promoter-derived transcript,  $\alpha$ SMA, and procollagen type I in the *Ecm1*:FLAG-infected livers compared to GFP controls at 16 weeks post the feeding of western diet and alternate drinking of 10% to 20% ethanol. Data were represented as means  $\pm$  SEM ( $n=4$ /group). \*\* $p < 0.01$ ; \* $p < 0.05$ . Student *t* test. Scale bar: 200  $\mu$ m. Graphs are quantification of stained areas based on image analysis of at least 10 random fields ( $\times 200$  magnification) per liver. (D) Decreases in hepatic hydroxyproline content were also found in the *Ecm1*:FLAG-infected livers compared to GFP controls ( $n=4$ /group). Data are means  $\pm$  SEM. \* $p < 0.05$ . Student *t* test. (E) Western blotting indicated less deregulation of *Hnf4 $\alpha$*  in the *Ecm1*:FLAG expressing livers ( $n=4$ ) than the GFP controls ( $n=4$ ) during the WDA-induced liver injury. Abbreviations: CTGF, connective tissue growth factor; ECM1, extracellular matrix protein 1;  $\alpha$ SMA,  $\alpha$ -smooth muscle actin.

in the WDA model that involves the feeding of western diet in combination with 10%–20% alcohol alternate drinking for 16 weeks in mice. This model is suitable for studying TGF $\beta$  and *Hnf4 $\alpha$*  deregulation in the setting of ALD since it recapitulates the inflammatory, fibrotic, and gene expression aspects of human AH.<sup>[13]</sup> We have demonstrated the antagonistic effects of *Hnf4 $\alpha$*  on TGF $\beta$ /SMAD3 signaling to regulate *Ctgf* expression.<sup>[37]</sup> To understand the effects of ectopic *Ecm1* on the expression of *Ctgf* and *Hnf4 $\alpha$*  during alcohol-associated fibrosis, we transduced AAV8-*Ecm1*:FLAG into mice and challenged them with the WDA model. As shown in Figure 6A, ectopic expression of *Ecm1* effectively suppressed *Ctgf* expression by 39.11%, *Hnf4 $\alpha$*  p2 transcript (*Hnf4 $\alpha$ -p2*) by 49.03%,  $\alpha$ SMA by 61.05%, and procollagen type I by 52.13%. Downregulation of *Ctgf*,  $\alpha$ SMA, and collagen type I proteins in AAV8-*Ecm1*:FLAG infected livers was observed in western blotting, densitometric analysis, and IHC (Figure 6B, C). AAV8-*Ecm1*:FLAG-attenuated fibrosis was also supported by the decreased levels of hepatic hydroxyproline (Figure 6D). Moreover, IHC and Western blot analyses demonstrated higher numbers of *Hnf4 $\alpha$* -positive hepatocytes and higher levels of this transcription factor when *Ecm1* was ectopically expressed (Figure 6C, E). These results indicate that forced *Ecm1* expression is hepatoprotective and reduces *Ctgf* upregulation, *Hnf4 $\alpha$*  deregulation, and fibrotic response in the WDA model.

## DISCUSSION

DR is associated with liver fibrosis in advanced chronic liver disease.<sup>[1]</sup> The DR process in cholangiopathies such as PSC and PBC involves the proliferation of cholangiocytes, whereas hepatic progenitor/oval cells are activated in the form of DR as part of regenerative processes that may supply new hepatocytes or BDECs to the injured livers in advanced ALD.<sup>[16]</sup> Despite these disparities, common pathways mediated by factors such as TGF $\beta$  are activated to induce scarring and liver repair. For instance, TGF $\beta$  activation causes defective metabolic and synthetic functions in hepatocytes that express fetal isoforms from p2 promoter *Hnf4 $\alpha$*  in human AH.<sup>[36]</sup> On the other hand, TGF $\beta$ 2 expression correlates positively in patients with PSC/PBC, and its knockdown

reduces biliary fibrosis in *Mdr2*<sup>-/-</sup> mice.<sup>[38]</sup> Thus, profibrotic signals represent potential therapeutic targets to inhibit liver fibrosis.<sup>[39,40]</sup> So far, there is limited treatment available due to a lack of effective antifibrotic agents. This study highlighted antifibrotic function of ECM1 as a biological glue to inhibit DR and fibrosis during cholangiopathy and alcohol-associated liver injury.

Normal hepatic ECM consists of fibrillar components and basement membrane constituents in the space of Disse, which is located between hepatocytes and liver sinusoidal endothelial cells. This liver ECM configuration is unique in maintaining the fenestration of liver sinusoidal endothelial cells and the differentiated states of hepatocytes during homeostasis. HSC, the hepatic-specific pericytes that normally store vitamin A, are the principal cells responsible for producing the interstitial matrix in a healthy liver. HSC is activated and transformed into myofibroblast cells during liver fibrosis. Activated HSC and myofibroblast seem to lose ECM1 expression based on single-cell transcriptomics data sets for fibrotic niches of human liver cirrhosis<sup>[31]</sup> and CCl<sub>4</sub>-induced murine liver fibrosis.<sup>[32]</sup> The indispensability of the *Ecm1* gene has been demonstrated by genetic evidence from knockout mice that spontaneously upregulates TGF $\beta$ /SMAD signaling, exhibits HSC hyperactivation, develops spontaneous liver fibrosis, and dies at 2 months of age devoid of hepatocyte damage and inflammation.<sup>[12]</sup> In agreement with this observation, we reported an enhanced susceptibility of germline *Ecm1* knockouts to DDC-induced DR and liver fibrosis. *Ecm1* loss was common in virtually all tested liver injuries in this study, including cholangiopathy and alcohol-associated liver injury, suggesting a severely detrimental effect of its deficiency in promoting liver fibrosis and DR.

The modular structure of ECM1 determines its biological activities. Identifying ECM1 interactors and their associated networks/pathways represents a viable approach for determining the functions of this secreted protein at the cellular and tissue levels within the context of the entire organism. The N-terminal domain of ECM1a consists of alpha-helices, while the remaining three domains, namely serum albumin subdomain-like domains 2–4, are topologically comparable to the subdomain of the third serum albumin domain.<sup>[41]</sup> The 2 tandem repeat domains and the C-terminal domain contain a specific cysteine arrangement, C-(X<sub>12-38</sub>)-

CC-(X<sub>7-10</sub>)-C, typical of the helical double-loop structural motif, thereby contributing to protein-protein interactions. This specific motif may enable ECM1 to serve as a transporter protein and/or be involved in binding, growth, and/or differentiation factors. ECM1 interactors include integrins, which bind to ECM fibrils and associate with intracellular actin filaments through various cytoskeletal linker proteins to mechanically connect the intracellular and extracellular structures. The physical association of ECM1 with different integrin subtypes can give rise to nuanced effects, depending on the tissue and context. For instance, ECM1 associates with integrin  $\alpha$ X $\beta$ 2 or  $\beta$ 4 to help promote ovarian and gastric cancers,<sup>[42,43]</sup> whereas its interaction with integrin  $\alpha$ v inhibits Th17 cell development in experimental autoimmune encephalomyelitis.<sup>[19]</sup> Integrin  $\alpha$ v can also form heterodimers with different  $\beta$  subunits ( $\beta$ 1,  $\beta$ 3,  $\beta$ 5,  $\beta$ 6, and  $\beta$ 8) to promote tissue fibrosis. ECM1 association with integrin  $\alpha$ v has been proposed as a key mechanism for the stabilization of TGF $\beta$  in normal livers.<sup>[6,12]</sup> Integrin  $\alpha$ v $\beta$ 6 is unique because the *Itg $\beta$ 6* gene is specifically expressed in epithelial cells and mediates the activation of TGF $\beta$ 1 and TGF $\beta$ 3 by recognizing the RGD motif in LAP via mechanical stress. Recently, integrin  $\alpha$ v $\beta$ 6 has been shown to promote TGF $\beta$ 2 activation by recognizing a related but divergent integrin-recognition motif.<sup>[44]</sup> We and others have demonstrated that integrin  $\alpha$ v $\beta$ 6 promotes hepatic progenitor cell activation and DR, and its inhibition blocks TGF $\beta$  activation and fibrosis during liver injury.<sup>[9]</sup> It is easy to postulate that ectopic expression of *Ecm1* may sequester integrins, such as  $\alpha$ v $\beta$ 6, from recognition to LAP and blocks TGF $\beta$  activation, thereby reducing DR and biliary fibrosis during the DDC or ANIT-induced liver injury.

Another important finding of this study was the identification of ECM1 as a CTGF-binding protein. Both ECM1 and CTGF are extracellular signaling modulators. CTGF is often co-overexpressed with TGF $\beta$  in a diverse variety of fibrotic disorders, potentiates TGF $\beta$  signaling by binding to and enhancing the presentation of this profibrotic master regulator to cognate receptors, and its overexpression renders the liver susceptibility to fibrosis.<sup>[8,45]</sup> CTGF protein contains a mosaic protein structure with binding sites for growth factors, cell-surface receptors, extracellular ligands, and matrix structural proteins. Through these interactions, CTGF regulates cell adhesion, migration, proliferation, differentiation, angiogenesis, and fibrosis. The SLIT2/ROBO1 pathway has been known to promote liver fibrosis. CTGF physically binds to the SLIT2 ligand and potentiates the profibrotic ROBO1 signaling in activated HSC.<sup>[15]</sup> In addition, it can function together with integrin  $\alpha$ v $\beta$ 6 to promote TGF $\beta$  activation, DR, and biliary fibrosis.<sup>[9]</sup> This study demonstrated the interaction between CTGF and ECM1 via the CT motif, which is known to form cysteine knots critical for the induction of

dimerization and receptor signaling mediated by growth factors and extracellular ligands in the cysteine knot superfamily.<sup>[46]</sup> Through this CT motif, CTGF can act as an adaptor linking fibronectin-enriched matrix with various subtypes of integrins (eg,  $\alpha$ 5 $\beta$ 1 and  $\alpha$ v $\beta$ 3) and promote HSC adhesion.<sup>[18,20,47]</sup> Therefore, it is conceivable that ECM1 can bind to the CT motif and prevent the availability of CTGF to profibrotic signaling from SLIT2/ROBO1 pathway, TGF $\beta$ , fibronectin, and  $\alpha$ v $\beta$ 6. These inhibitions caused by ECM1-mediated sequestration of CTGF through interaction with the CT motif likely contribute to attenuated activation of HSC and DR as well as reduced liver fibrosis during injury.

In summary, ECM1 is a potent antifibrotic factor and can sequester profibrotic factors, thereby inhibiting  $\alpha$ v $\beta$ 6-mediated TGF $\beta$  activation. It is often downregulated during chronic liver injury. Hepatoprotective effects of restored expression of ECM1 protein against TGF $\beta$  activation, DR, and liver fibrosis underscore the promise of this antifibrotic molecule in treatment of chronic liver diseases such as cholangiopathy and AH.

#### DATA AVAILABILITY STATEMENT

All data generated or analyzed during this study are included in this published article and its Supplemental Information files.

#### AUTHOR CONTRIBUTIONS

Chunbao Sun, Junmei Zhou, Bing Sun, Xiao-Ming Yin, Chen Ling, Bryon Petersen, and Liya Pi designed this study. Chunbao Sun, Sreenivasulu Basha, Weiguo Fan, Tian Tian, Brady Jin-Smith, Joshua Barkin, Hanhui Xie, and Liya Pi performed the experiments and analyzed the data. Liya Pi wrote the article. All authors have read the draft of this article, suggested improvements, and approved the final version.

#### FUNDING INFORMATION

This study is supported by the National Institutes of Health NIAAA RO1AA028035 grant awarded to Liya Pi.

#### CONFLICTS OF INTEREST

The authors have no conflicts to report.

#### REFERENCES

1. Marakovits C, Francis H. Unraveling the complexities of fibrosis and ductular reaction in liver disease: Pathogenesis, mechanisms, and therapeutic insights. *Am J Physiol Cell Physiol*. 2024; 326:C698–706.
2. Sancho-Bru P, Altamirano J, Rodrigo-Torres D, Coll M, Millan C, Jose Lozano J, et al. Liver progenitor cell markers correlate with liver damage and predict short-term mortality in patients with alcoholic hepatitis. *Hepatology*. 2012;55:1931–41.
3. Ren C, Paronetto F, Mak KM, Leo MA, Lieber CS. Cytokeratin 7 staining of hepatocytes predicts progression to more severe fibrosis in alcohol-fed baboons. *J Hepatol*. 2003;38:770–5.
4. Atkinson SR, Aly M, Remih K, Tyson LD, Guldiken N, Goldin R, et al. Serum keratin 19 (CYFRA21-1) is a prognostic biomarker in severe alcoholic hepatitis. *Liver Int*. 2022;42:1049–57.



5. Dewidar B, Meyer C, Dooley S, Meindl-Beinker N. TGF-beta in hepatic stellate cell activation and liver fibrogenesis—Updated 2019. *Cells*. 2019;8:1419.
6. Li Y, Fan W, Link F, Wang S, Dooley S. Transforming growth factor beta latency: A mechanism of cytokine storage and signalling regulation in liver homeostasis and disease. *JHEP Rep*. 2022;4:100397.
7. Fontana L, Chen Y, Prijatelj P, Sakai T, Fassler R, Sakai LY, et al. Fibronectin is required for integrin alphavbeta6-mediated activation of latent TGF-beta complexes containing LTBP-1. *FASEB J*. 2005;19:1798–808.
8. Abreu JG, Ketpura NI, Reversade B, De Robertis EM. Connective-tissue growth factor (CTGF) modulates Cell signaling by BMP and TGF-beta. *Nat Cell Biol*. 2002;4:599–604.
9. Pi L, Robinson PM, Jorgensen M, Oh SH, Brown AR, Weinreb PH, et al. Connective tissue growth factor and integrin alphavbeta6: A new pair of regulators critical for ductular reaction and biliary fibrosis in mice. *Hepatology*. 2015;61:678–91.
10. Ramazani Y, Knops N, Elmonem MA, Nguyen TQ, Arcolino FO, van den Heuvel L, et al. Connective tissue growth factor (CTGF) from basics to clinics. *Matrix Biol*. 2018;68-69:44–66.
11. Hamada T, McLean WH, Ramsay M, Ashton GH, Nanda A, Jenkins T, et al. Lipoid proteinosis maps to 1q21 and is caused by mutations in the extracellular matrix protein 1 gene (ECM1). *Hum Mol Genet*. 2002;11:833–40.
12. Fan W, Liu T, Chen W, Hammad S, Longerich T, Hausser I, et al. ECM1 prevents activation of transforming growth factor beta, hepatic stellate cells, and fibrogenesis in mice. *Gastroenterology*. 2019;157:1352–67 e1313.
13. Schonfeld M, O'Neil M, Villar MT, Artigues A, Averilla J, Gunewardena S, et al. A western diet with alcohol in drinking water recapitulates features of alcohol-associated liver disease in mice. *Alcohol Clin Exp Res*. 2021;45:1980–93.
14. Joshi N, Ray JL, Kopec AK, Luyendyk JP. Dose-dependent effects of alpha-naphthylisothiocyanate disconnect biliary fibrosis from hepatocellular necrosis. *J Biochem Mol Toxicol*. 2017;31:1–7.
15. Pi L, Sun C, Jn-Simon N, Basha S, Thomas H, Figueroa V, et al. CCN2/CTGF promotes liver fibrosis through crosstalk with the Slit2/Robo signaling. *J Cell Commun Signal*. 2023;17:137–50.
16. Pi L, Ding X, Jorgensen M, Pan JJ, Oh SH, Pintilie D, et al. Connective tissue growth factor with a novel fibronectin binding site promotes cell adhesion and migration during rat oval cell activation. *Hepatology*. 2008;47:996–1004.
17. Pi L. The Role of Connective Tissue Growth Factor (CTGF) in Oval Cell Aided Liver Regeneration in the 2-AAF/PHx Model UMI. University of Florida Gainesville; 1995.
18. Hoshijima M, Hattori T, Inoue M, Araki D, Hanagata H, Miyauchi A, et al. CT domain of CCN2/CTGF directly interacts with fibronectin and enhances cell adhesion of chondrocytes through integrin alpha5beta1. *FEBS Lett*. 2006;580:1376–82.
19. Su P, Chen S, Zheng YH, Zhou HY, Yan CH, Yu F, et al. Novel function of extracellular matrix protein 1 in suppressing Th17 cell development in experimental autoimmune encephalomyelitis. *J Immunol*. 2016;197:1054–64.
20. Gao R, Brigstock DR. Connective tissue growth factor (CCN2) induces adhesion of rat activated hepatic stellate cells by binding of its C-terminal domain to integrin alpha(v)beta(3) and heparan sulfate proteoglycan. *J Biol Chem*. 2004;279:8848–55.
21. Hendsi H, Barbe MF, Safadi FF, Monroy MA, Popoff SN. Integrin mediated adhesion of osteoblasts to connective tissue growth factor (CTGF/CCN2) induces cytoskeleton reorganization and cell differentiation. *PLoS One*. 2015;10:e0115325.
22. Sun Y, Vandenbriele C, Kauskot A, Verhamme P, Hoylaerts MF, Wright GJ. A human platelet receptor protein microarray identifies the high affinity immunoglobulin E receptor subunit alpha (FcepsilonR1alpha) as an activating platelet endothelium aggregation receptor 1 (PEAR1) ligand. *Mol Cell Proteomics*. 2015;14:1265–74.
23. Patsenker E, Popov Y, Stickel F, Jonczyk A, Goodman SL, Schuppan D. Inhibition of integrin alphavbeta6 on cholangiocytes blocks transforming growth factor-beta activation and retards biliary fibrosis progression. *Gastroenterology*. 2008;135:660–70.
24. Jing J, Li P, Li T, Sun Y, Guan H. RNA interference targeting connective tissue growth factor inhibits the transforming growth factor-beta 2 induced proliferation in human tenon capsule fibroblasts. *J Ophthalmol*. 2013;2013:354798.
25. Trinchet JC, Gerhardt MF, Balkau B, Munz C, Poupon RE. Serum bile acids and cholestasis in alcoholic hepatitis. Relationship with usual liver tests and histological features. *J Hepatol*. 1994;21:235–40.
26. Ye L, Ziesch A, Schneider JS, Ofner A, Niess H, Denk G, et al. The inhibition of YAP signaling prevents chronic biliary fibrosis in the Abcb4(-/-) model by modulation of hepatic stellate cell and bile duct epithelium cell pathophysiology. *Aging Dis*. 2024;15:338–56.
27. Richter ML, Deligiannis IK, Yin K, Danese A, Lleshi E, Coupland P, et al. Single-nucleus RNA-seq. 2 reveals functional crosstalk between liver zonation and ploidy. *Nat Commun*. 2021;12:4264.
28. Yang W, He H, Wang T, Su N, Zhang F, Jiang K, et al. Single-cell transcriptomic analysis reveals a hepatic stellate cell-activation roadmap and myofibroblast origin during liver fibrosis in mice. *Hepatology*. 2021;74:2774–90.
29. Payen VL, Lavergne A, Alevra Sarika N, Colonval M, Karim L, Deckers M, et al. Single-cell RNA sequencing of human liver reveals hepatic stellate cell heterogeneity. *JHEP Rep*. 2021;3:100278.
30. Su Q, Kim SY, Adewale F, Zhou Y, Aldler C, Ni M, et al. Single-cell RNA transcriptome landscape of hepatocytes and non-parenchymal cells in healthy and NAFLD mouse liver. *iScience*. 2021;24:103233.
31. Ramachandran P, Dobie R, Wilson-Kanamori JR, Dora EF, Henderson BEP, Luu NT, et al. Resolving the fibrotic niche of human liver cirrhosis at single-cell level. *Nature*. 2019;575:512–8.
32. Dobie R, Wilson-Kanamori JR, Henderson BEP, Smith JR, Matchett KP, Portman JR, et al. Single-cell transcriptomics uncovers zonation of function in the mesenchyme during liver fibrosis. *Cell Rep*. 2019;29:1832–47. e1838.
33. Fickert P, Stoger U, Fuchsichler A, Moustafa T, Marschall HU, Weiglein AH, et al. A new xenobiotic-induced mouse model of sclerosing cholangitis and biliary fibrosis. *Am J Pathol*. 2007;171:525–36.
34. Santamaria E, Rodriguez-Ortigosa CM, Uriarte I, Latasa MU, Urtasun R, Alvarez-Sola G, et al. The epidermal growth factor receptor ligand amphiregulin protects from cholestatic liver injury and regulates bile acids synthesis. *Hepatology*. 2019;69:1632–47.
35. Sullivan BP, Weinreb PH, Violette SM, Luyendyk JP. The coagulation system contributes to alphaVbeta6 integrin expression and liver fibrosis induced by cholestasis. *Am J Pathol*. 2010;177:2837–49.
36. Argemi J, Latasa MU, Atkinson SR, Blokhin IO, Massey V, Gue JP, et al. Defective HNF4alpha-dependent gene expression as a driver of hepatocellular failure in alcoholic hepatitis. *Nat Commun*. 2019;10:3126.
37. Zhou J, Sun X, Yang L, Wang L, Ran G, Wang J, et al. Hepatocyte nuclear factor 4alpha negatively regulates connective tissue growth factor during liver regeneration. *FASEB J*. 2020;34:4970–83.
38. Dropmann A, Dooley S, Dewidar B, Hammad S, Dediulia T, Werle J, et al. TGF-beta2 silencing to target biliary-derived liver diseases. *Gut*. 2020;69:1677–90.
39. Monga SP, Nejak-Bowen K. Ductular reaction and liver regeneration: Fulfilling the prophecy of Prometheus!. *Cell Mol Gastroenterol Hepatol*. 2023;15:806–808.

40. Aseem SO, Jalan-Sakrikar N, Chi C, Navarro-Corcuera A, De Assuncao TM, Hamdan FH, et al. Epigenomic evaluation of cholangiocyte transforming growth factor-beta signaling identifies a selective role for histone 3 lysine 9 acetylation in biliary fibrosis. *Gastroenterology*. 2021;160:889–905 e810.
41. Smits P, Ni J, Feng P, Wauters J, Van Hul W, Boutaibi ME, et al. The human extracellular matrix gene 1 (ECM1): Genomic structure, cDNA cloning, expression pattern, and chromosomal localization. *Genomics*. 1997;45:487–95.
42. Yin H, Wang J, Li H, Yu Y, Wang X, Lu L, et al. Extracellular matrix protein-1 secretory isoform promotes ovarian cancer through increasing alternative mRNA splicing and stemness. *Nat Commun*. 2021;12:4230.
43. Gan L, Meng J, Xu M, Liu M, Qi Y, Tan C, et al. Extracellular matrix protein 1 promotes cell metastasis and glucose metabolism by inducing integrin beta4/FAK/SOX2/HIF-1alpha signaling pathway in gastric cancer. *Oncogene*. 2018;37:744–55.
44. Le VQ, Zhao B, Ramesh S, Toohey C, DeCosta A, Mintseris J, et al. A specialized integrin-binding motif enables proTGF-beta2 activation by integrin alphaVbeta6 but not alphaVbeta8. *Proc Natl Acad Sci USA*. 2023;120:e2304874120.
45. Tong Z, Chen R, Alt DS, Kemper S, Perbal B, Brigstock DR. Susceptibility to liver fibrosis in mice expressing a connective tissue growth factor transgene in hepatocytes. *Hepatology*. 2009;50:939–47.
46. Pi L, Shenoy AK, Liu J, Kim S, Nelson N, Xia H, et al. CCN2/CTGF regulates neovessel formation via targeting structurally conserved cystine knot motifs in multiple angiogenic regulators. *FASEB J*. 2012;26:3365–79.
47. Gao R, Brigstock DR. A novel integrin alpha5beta1 binding domain in module 4 of connective tissue growth factor (CCN2/CTGF) promotes adhesion and migration of activated pancreatic stellate cells. *Gut*. 2006;55:856–62.

**How to cite this article:** Sun C, Weiguo F, Basha S, Tian T, Jin-Smith B, Barkin J, et al. Extracellular matrix protein 1 binds to connective tissue growth factor against liver fibrosis and ductular reaction. *Hepatol Commun*. 2024;8:e0564. <https://doi.org/10.1097/HC9.000000000000564>